Chapter 17

Localized Surface Plasmon Resonance for Optical Fiber-Sensing Applications

Pedro J. Rivero, Javier Goicoechea and

Francisco J. Arregui

Additional information is available at the end of the chapter

http://dx.doi.org/10.5772/67544

Abstract

It is well known that optical fiber sensors have attracted the attention of scientific community due to its intrinsic advantages, such as lightweight, small size, portability, remote sensing, immunity to electromagnetic interferences and the possibility of multiplexing several signals. This field has shown a dramatic growth thanks to the creation of sensitive thin films onto diverse optical fiber configurations. In this sense, a wide range of optical fiber devices have been successfully fabricated for monitoring biological, chemical, medical or physical parameters. In addition, the use of nanoparticles into the sensitive thin films has resulted in an enhancement in the response time, robustness or sensitivity in the optical devices, which is associated to the inherent properties of nanoparticles (high surface area ratio or porosity). Among all of them, the metallic nanoparticles are of great interest for sensing applications due to the presence of strong absorption bands in the visible and near-infrared regions, due to their localized surface plasmon resonances (LSPR). These optical resonances are due to the coupling of certain modes of the incident light to the collective oscillation of the conduction electrons of the metallic nanoparticles. The LSPR extinction bands are very useful for sensing applications as far as they can be affected by refractive index variations of the surrounding medium of the nanoparticles, and therefore, it is possible to create optical sensors with outstanding properties such as high sensitivity and optical self-reference. In this chapter, the attractive optical properties of metal nanostructures and their implementation into different optical fiber configuration for sensing or biosensing applications will be studied.

Keywords: LSPR, optical fiber, sensing applications

1. Introduction

In this highly technological era in which we live, we are involved in a virtuous circle in which new machines, systems and devices are continuously created. This technological evolution has produced an evident improvement in our lifestyle, making our lives easier and more comfortable, and also contributing to the wealth distribution in the world. For a high number of those new systems, devices and new applications, sensors play a key role as far as they provide the link between the real-world and the technological devices. Sensors are much more effective than our five senses, and they can provide information not only about taste, smell or touch, but also about the presence of explosives [1], certain bacteria, viruses and biological markers [2, 3], magnetic fields, radiation, traces of pollutants [4] and many other applications. Consequently, there is a continuous effort in the research of new sensing devices that allow us to get information of our environment and consequently use this information to improve the existing devices or even the discovery of new applications. There has been a dramatic evolution starting from the classic analog sensors used for decades and decades to the current electronic smart sensors and other advanced sensing devices such as optical fiber sensors (**Figure 1**).

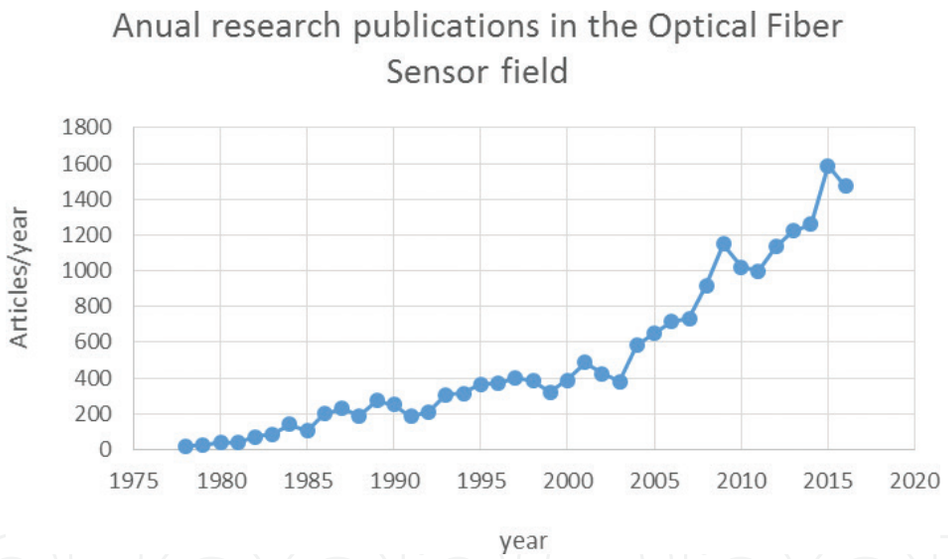

Figure 1. Number of published articles in international research journals with the words "Optical," "Fiber" and "Sensor" in their title, abstract or keywords (source: Scopus database).

The very first optical sensors were simple, mostly based on physical alterations of the natural waveguide structure of a regular optical fiber. The irruption of more advanced optical structures, such as fiber Bragg-gratings (FBGs), long-period gratings (LPGs), photonic crystal fibers (PCFs) and D-shape fibers opened the door to a new generation of optical fiber sensors based on interferometry, optical resonances, etc. Moreover, the combination of those families of optical fiber structures with coatings has made possible the apparition of more advanced optical fiber sensors.

As the sensitive coatings have been engineered, they have become more controllable and complex, and new materials have been incorporated to these devices, such as nanoparticles,

http://dx.doi.org/10.5772/67544

fluorescent dyes, proteins, antibodies and aptamers. Additionally, the control of the structure of the coatings at the nanoscale level allows the ability to tailor at the molecular level of the composition and structure of the sensitive coatings. These nanoscaled materials have a special attraction because there are new phenomena observed when the matter is downscaled to this level. This is the case of the outstanding luminescence properties observed in semiconductor chalcogenide nanoparticles (e.g., CdTe, CdS) due to the exciton quantum confinement that has been widely used for sensor application [5]. Among these nanostructured materials, metallic nanoparticles have also been widely used because they show a very special optical resonance phenomenon known as localized surface plasmon resonance (LSPR). When light is propagated through a medium that contains certain metallic nanoparticles, the electrical field oscillation induced by light affects to the free electrons in the nanoparticles. There is a resonance condition in which the energy present in the electromagnetic wave is coupled to the electrons in the nanoparticle inducing their collective oscillation. Consequently, metallic nanoparticle dispersions show vivid and intense colors in the visible region of the electromagnetic spectrum. This resonance condition can be affected significantly by the composition of the metallic nanoparticles, by their shape and by the alteration of the effective refractive index of the medium surrounding the nanoparticle, typically in a radius of a few nanometers [6]. As a consequence, there has been a great research effort in the development of sensitive functionalization of noble metal nanoparticles in order to get improved sensing devices. The intensity and the wavelength position of LSPR attenuation bands may be affected by very small variations of the surrounding medium, and this can be used for the development of highly sensitive devices, talking even about single-molecule detection limits. LSPR has also been combined with complementary molecular identification techniques such as surface-enhanced Raman spectroscopy (SERS) [7].

Some authors have proposed different approaches using the LSPR of noble metallic nanoparticles in the research of new optical fiber sensors. Such optical fiber sensors combine the LSPR technology with the classical advantages of optical fiber sensors, such as lightweight devices, electromagnetic immunity, biocompatibility and remote sensing. Thus, taking the advantages of the LSPR resonances, it is possible to create a new generation of optical fiber sensors.

In this chapter, we will present a thorough review of the state of the art of LPSR-based optical fiber sensors. Firstly, the most used synthesis techniques of metallic nanoparticles and their possible immobilization approaches into different thin films are presented. Afterward, it will be presented the main applications for sensing physical parameters (refractive index, humidity, etc.), chemical parameters (pH, heavy metal ions, volatile and harmful compounds) and biological parameters (blood sugar, proteins, antigens and antibodies, etc.).

2. Introduction to the synthesis of metal nanoparticles

One of the most explored characteristics of the noble metal nanoparticles (essentially silver, gold or copper) is the localized surface plasmon resonance (LSPR), which is the frequency at which conduction electrons collectively oscillate in response to the alternating electric field

of an incident electromagnetic radiation. As a result, an intense absorption band in the visible region with a specific coloration of the resultant nanoparticles is obtained [8, 9]. A relevant aspect in the synthesis of metal nanoparticles is that their optical properties present a great dependence with the resultant morphology. A good monitoring of the evolution of the LSPR wavelength position and the corresponding color formation makes possible to obtain nanoparticles with a desirable shape and size [10–12]. A fine control of several parameters (shape, size, surface functionalization or interparticle distance) is a challenging goal, and a large number of reports have been published with the aim to synthesize metal nanoparticles with a desired morphology, mainly for plasmonic or sensing applications [13–17].

Among all the synthetic methodologies, one of the most frequently used methods is based on the chemical reduction in metallic salts (mainly $AgNO_3$ or $HAuCl_4 \cdot 3H_2O$) by using a reducing agent, which is responsible for reducing the cationic metallic salts to produce the respective metal nanoparticles. In addition, an adequate protective agent is also used because it plays a dual role of preventing the agglomeration and maintaining the unaltered aggregation state of the metal nanoparticles. In this sense, Rivero et al. [18] presented a multicolor silver map with a long-term stability by means of a fine control of the molar ratio between both protective agent (polyacrylate, PAA) and reducing agent (dimethylaminoborane, DMAB), enabling a wide range of colors (yellow, orange, red, violet, blue, green, brown) and tunable shape and size. **Figure 2a** shows a multicolor silver map, which is formed by 56 different combinations of protective agent concentration and reducing/loading agent ratio. **Figure 2b** depicts the evolution of the LSPR absorption bands as a function of variable DMAB molar concentration.

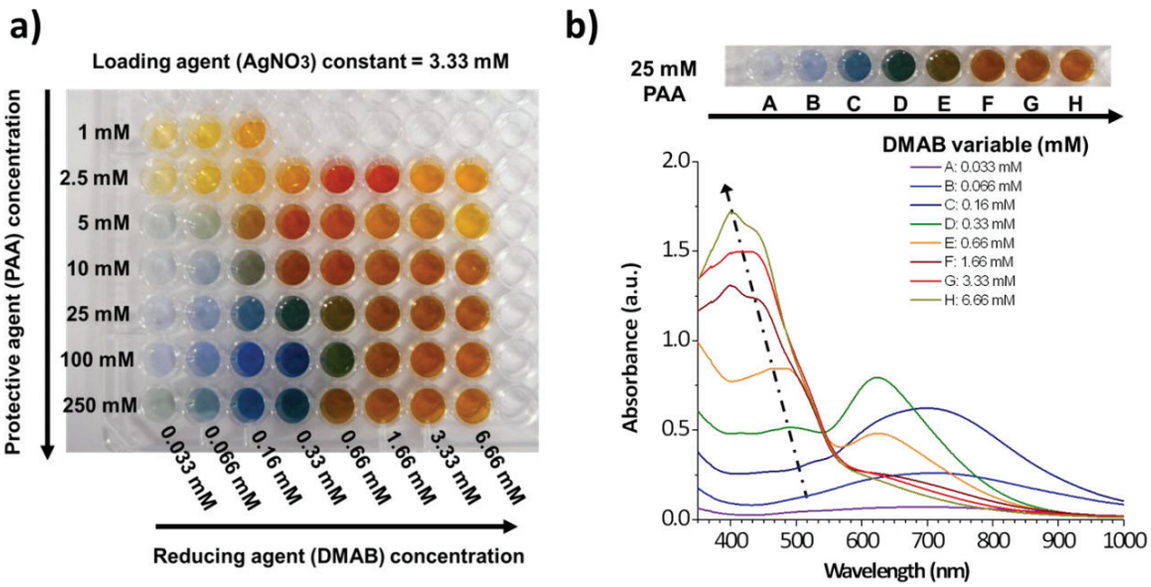

Figure 2. (a) Photograph of multicolor silver map obtained as function of variable protective (PAA) and reducing (DMAB) agents; (b) UV-vis spectra of silver solutions at a constant DMAB concentration. They are prepared with different DMAB molar concentrations at a constant PAA concentration of 25 mM (fifth line of the multicolor silver map of **Figure 1a**). Reprinted with permission from Ref. [18]. Copyright (2013) Springer.

3. Immobilization techniques of metal nanoparticles

First of all, a good immobilization of the metallic nanoparticles onto the optical fiber is necessary because this aspect is the most relevant key point for a further sensing application. The most used techniques for an adequate immobilization of the resultant metal nanoparticles are the layer-by-layer (LbL) assembly, sol-gel process or silanization process. All these processes offer a wide range of advantages, such as high versatility, easiness of implementation and simplicity. In addition, these techniques can easily incorporate metal nanoparticles in the resultant structure. However, it is necessary to remark that it can be found in the bibliography other alternative methods such as chemisorption, photodeposition or in situ synthesis of metal nanoparticles onto optical fiber, which can be also used for LSPR-sensing technology.

3.1. The sol-gel process

The sol-gel process is a synthetic route for preparing inorganic or hybrid inorganic-organic materials with a high purity through chemical reactions (known as hydrolysis, condensation and polycondensation) from a specific metal alkoxide [19–22]. All the chemical reactions follow the same evolution from a sol, a colloidal suspension of solid particles in a liquid, to produce a gel, a substance that contains a continuous solid skeleton enclosing a continuous liquid phase. A remarkable aspect is that the sol-gel process is a simple wet synthetic route, which can be easily used for loading other chemical agents. In this sense, metallic ions (precedent from metal inorganic salts) can be reduced in a later step to metal nanoparticles or well nanoparticles with a desired morphology can be perfectly introduced into the inorganic matrix during the polycondensation stage [23–25]. In addition, an important benefit is that sol-gel reactions do not employ extreme reaction conditions because the reactions take place at room or low temperature and require only moderate temperature to cure the gel.

Finally, once the sol-gel precursor is prepared and aged for a specific period of time, the substrate (i.e., optical fiber) is immersed into it using the dip-coating technique. After a fixed period of time, it is pulled out from the gel by using a determined extracting speed. Then, the substrate is dried during a fixed time and some additional processing steps can be included such as a heat treatment at controlled conditions of temperature and pressure. These steps can be repeated until the coating has acquired the desired thickness. In **Figure 3**, a summary of all the steps involved in the sol-gel technology (hydrolysis, condensation, polycondensation) (**Figure 3a**) and the critical parameters involved in the dip-coating technique (**Figure 3b**) are presented, respectively.

3.2. The layer-by-layer (LbL) assembly

Other deposition technique for immobilizing the metallic nanoparticles into thin films is the layer-by-layer (LbL) assembly, being one of the most used methods in the nanoscale level for its simplicity and versatility in comparison with other techniques [26]. In addition, other important advantage is the easiness for scaling-up with a precise control of the resultant

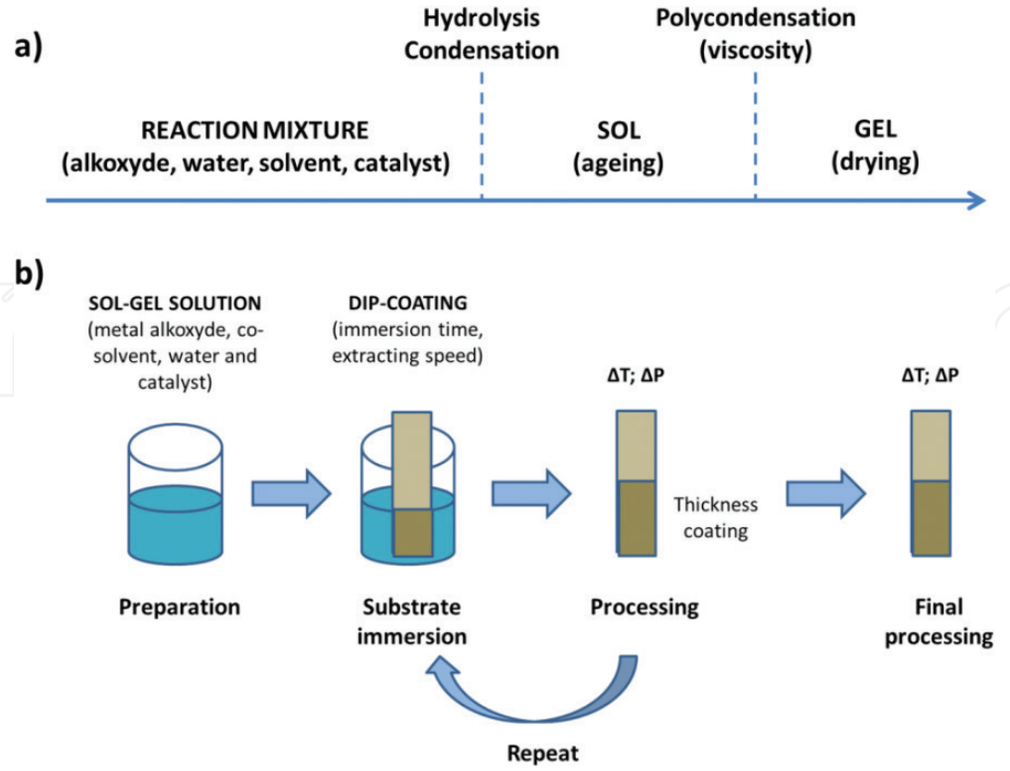

Figure 3. (a) Schematic representation of the different steps involved in the sol-gel process; (b) parameters to control in the dip-coating deposition technique.

thickness. The basis of this method is the electrostatic attraction between aqueous polyelectrolyte solutions of opposite charge, known as polycation (positive charge) and polyanion (negative charge), respectively. It is important to note that both polycations and polyanions overlap each other at the molecular level, and this produces a homogeneous optical material [27]. One of the main advantages of using polyelectrolytes is that their linear charge density can be varied over a wide range by simple adjustments of the pH or ionization degree of the dipping polyelectrolyte solutions [28, 29].

Other important advantage is that these polyelectrolytes can be used as protective agents of the metal nanoparticles. The encapsulating agent plays an important role for the synthesis of nanoparticles with a specific morphology because it limits the growth of the particles, directs their shape and provides colloidal stability [18]. Due to this, several works have been focused on the fabrication of thin films based on the incorporation of different shaped gold and silver nanoparticles using several types of polyelectrolytes [30–32]. A novel approach known as layer-by-layer embedding (LbL-E) deposition technique is based on a successive incorporation of metal nanoparticles with a well-defined morphology into LbL films, as it can be appreciated in **Figure 4**. More details about this deposition technique can be found in Refs. [31, 32].

Alternatively, other approach for incorporating metallic nanoparticles into LbL thin films is based on in situ chemical reduction from metal ions to metal nanoparticles. In order to perform this synthetic route, it is necessary to obtain a source of metal ions known as loading

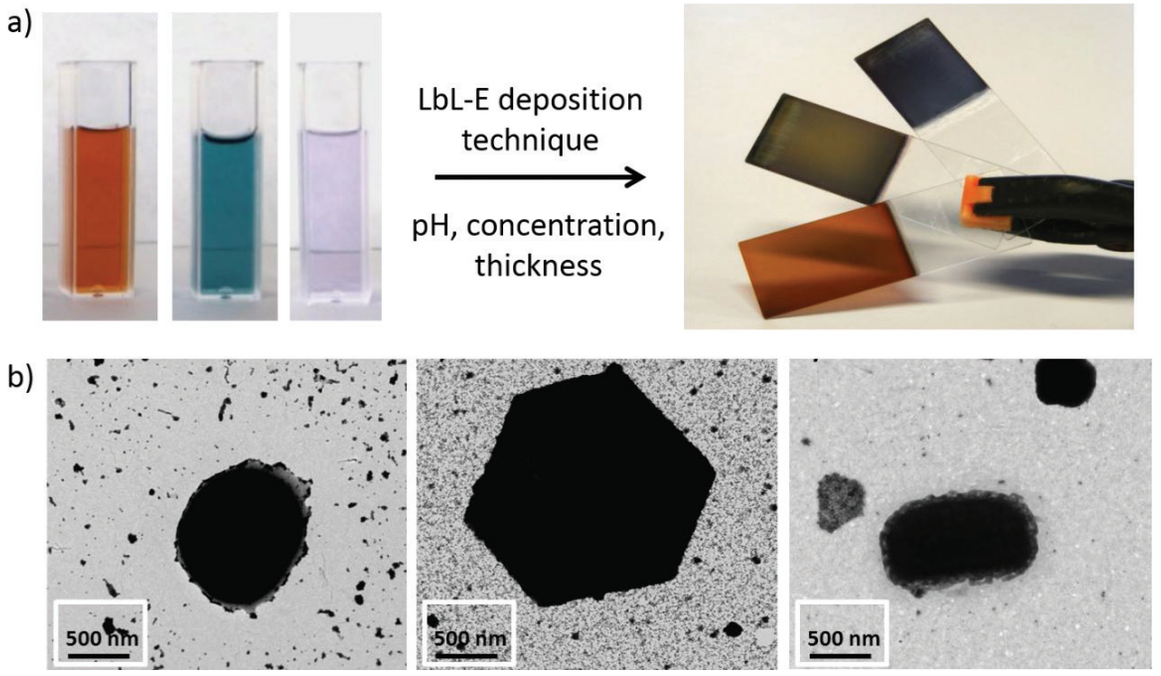

Figure 4. (a) Synthesis of silver nanoparticles with variable colors and their incorporation into polymeric thin films using LbL-E deposition technique; (b) TEM image of the AgNPs with a spherical shape (orange coloration), hexagonal shape (green coloration) and rod shape (violet coloration). Reprinted with permission from Refs. [32, 33]. Copyright (2013) Springer.

solution and a reducing solution, which is used for the chemical reduction of the metal ions. In this sense, once the metal ions have been successfully immobilized in the resultant LbL film, a further chemical reduction in the metal ions to zerovalent metal nanoparticles is performed when LbL films are immersed in a specific reducing solution. This approach based on in situ chemical reduction of the metal ions to nanoparticles into a previously host matrices used as a template can be called in situ synthesis (ISS) process. According to this, several articles can be found in the references using different loading/reducing agents as well as weak or strong polyelectrolytes in the resultant LbL films, respectively [33, 34].

3.3. Alternative methods for the immobilization of the metal nanoparticles

Other alternative methods for the immobilization of the nanoparticles consist of a previous pretreatment of the unclad surface of the optical fiber and a further silanization process to immobilize the metallic nanoparticles. For this purpose, firstly, the substrate is immersed in a piranha solution (H_2O_2:H_2SO_4; 30%:70%) for a specific period of time between 30 min and 1 h. This step is of great importance because the glass of the fiber is hydrolyzed, making possible the creation of additional SiOH sites in the outer surface of the fiber. However, this solution is extremely dangerous and must be manipulated with extreme precaution. Then, the optical fiber is rigorously rinsed in ultrapure water and placed in an oven at 100°C for 1 h in order to stabilize the new SiOH sites onto the surface of the optical fiber, being the key point for a further chemical binding. According to this, the optical fiber is immersed in a specific ORMOSIL (organically modified silicate) solution, being the most used aminosilane as

well as mercaptosilane solution. These ORMOSILS are used to create a self-assembled layer onto the optical fiber surface, which is used to attach the metal nanoparticles with a desired shape by specific functional groups such mercapto (–SH) or amine ($–NH_2$) of the corresponding ORMOSIL. Once the nanoparticles have been successfully incubated and immobilized onto the fiber surface, the optical fibers are washed with ultrapure water to remove unbound nanoparticles.

An example of the optical fiber structure after immobilizing a specific type of nanoparticles such as gold nanorods (GNRs) can be appreciated in **Figure 5**. It can be appreciated as a thin silver layer is coated onto the end surface of fiber with the aim to make a reflective optical fiber sensor probe. Then, the silanization process is performed for a further attachment of the GNRs onto optical fiber core. Finally, the UV-vis spectrum of the GNRs shows two well-distinguished absorption bands related to the transversal plasmon resonance (530 nm) and longitudinal plasmon resonance (around 720 nm), respectively.

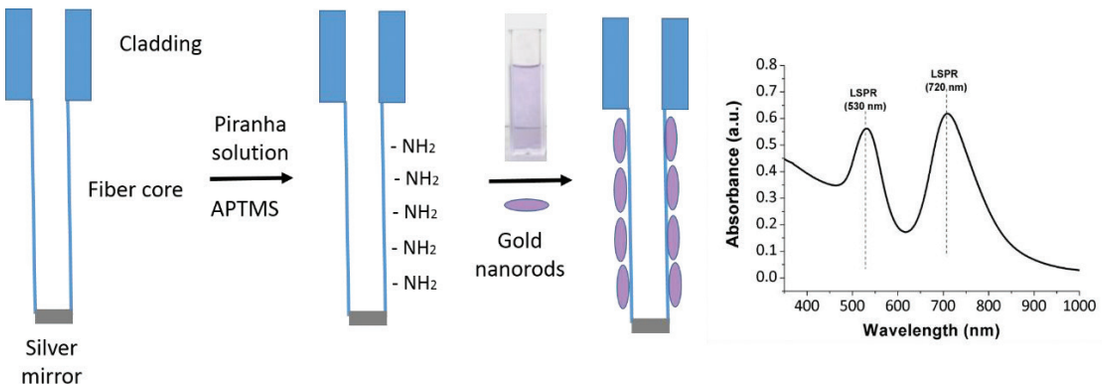

Figure 5. A schematic representation of the structure of LSPR-based optical fiber sensor after immobilization of GNRs using a silanization process.

4. Applications of the LSPR-based optical fiber sensors

In this section, once metal nanoparticles with a desired morphology have been successfully immobilized onto the optical fiber surface, potential applications of the plasmonic properties inherent to the nanoparticles are studied, specifically for sensing applications in the industry or biosensing applications in the field of clinical diagnosis or medicine. For all these purposes, the implementation of LSPR-based optical fiber sensors has attracted greater attention for all these potential applications. In the first subsection, optical fiber sensors for the detection of physical parameters such as relative humidity and refractive index are presented. In a second subsection, the design of optical fiber sensors is presented for the detection of wide variety of chemical parameters (i.e., pH, hydrogen peroxide, gases or heavy metals). Finally, optical fiber biosensors are presented for the detection of biochemical parameters (i.e., glucose, antigens, IgG) in the third subsection by using the LSPR technology.

4.1. Detection of physical parameters

4.1.1. Optical fiber refractometers

Refractometers are extensively used in fields as diverse as chemistry, biochemistry, food preservation, beverage industry or medicine to measure the surrounding medium refractive index (SMRI). In addition, they can be also combined with sensing coatings whose refractive index depends on the specific parameter under study [35, 36]. It is important to remark that different optical geometries have been studied with the aim to increase the sensitivity of the devices. However, optical fiber-based refractive index sensors are highly preferred for several applications where in situ and real-time monitoring is a key point. Due to this, recent works have demonstrated that the combination of nanodeposition techniques with optical fiber sensors is becoming a hot topic in the fabrication of thin-film-coated devices for measuring the refractive index.

As it was commented in Section 2, among all the deposition techniques at nanoscale level, one of the most used is the layer-by-layer assembly because it has the additional advantage of incorporating metal nanoparticles for plasmonic applications. In this sense, several articles related to both LbL assembly and metallic nanoparticles can be found in the references for measuring the refractive index [37–40]. According to this, Gouvêa et al. [37] have performed a dual growth kinetic study with the aim to evaluate the optimal deposition time as well as the optimal number of bilayers to fabricate a fiber optic reflection-based localized surface plasmon resonance sensor using LbL technique composed of PAMAM dendrimer/gold nanoparticles. Other interesting studies for the fabrication of optical fiber refractometers based on the successive incorporation of gold nanoparticles into LbL coatings are presented in Refs. [38, 39]. These works are based on the apparition of multiple absorption bands in the visible as a function of the thickness coating by using the LbL-E deposition technique, showing different sensitivity when the devices are exposed to variations of the refractive index from 1.33 to 1.42. In addition, as observed in Ref. [40], the utilization of both layer-by-layer polylectrolyte and metal nanoparticles within the polymeric composite films makes also possible to obtain a very high refractive index overlay with a significant sensitivity enhancement over ambient refractive index change, showing potential applications as biosensors. However, other alternative methods can be found in the references in order to immobilize the nanoparticles [41–52]. As an example, photodeposition technique has been used to immobilize AgNPs on the optical fiber end [41]. This LSPR-based optical fiber sensor has been exposed to different values of refractive index such as air (n = 1), deionized water (n = 1.33), ethanol (n = 1.36) and clove oil (n = 1.5). The experimental results indicate that there is change in the LSPR peak wavelength position when the refractive index is continuously increased (see **Figure 6**). In addition, a linear curve can be fitted according to the experimental data, showing a sensor sensitivity of 67.6 nm/RIU.

Other interesting work based on the incorporation of silver nanoparticles for the design of reflective LSPR-based optical fiber biosensors is presented in Ref. [42]. In this work, the synthesized AgNPs showed mostly a spherical shape with the peak located near 405 nm and with a particle diameter around 30 nm (see **Figure 7**). In addition, two parameters such as length of

sensing area and coating time have been optimized with the aim to enhance the sensitivity of the LSPR optical sensor. The sensitivity of the sensor probe to reflective indices was 387 nm/RIU, and the total peak wavelength shift was approximately of 30 nm for a RI ranges from 1.33 to 1.40, as it can be observed in **Figure 8**.

Other characteristic example is presented in Ref. [43], where gold nanoparticles with a specific shape (nanoflower) have been successfully immobilized onto U-bent plastic optical fiber (POF) by means of a process known as chemisorption, which consists of a specific reaction

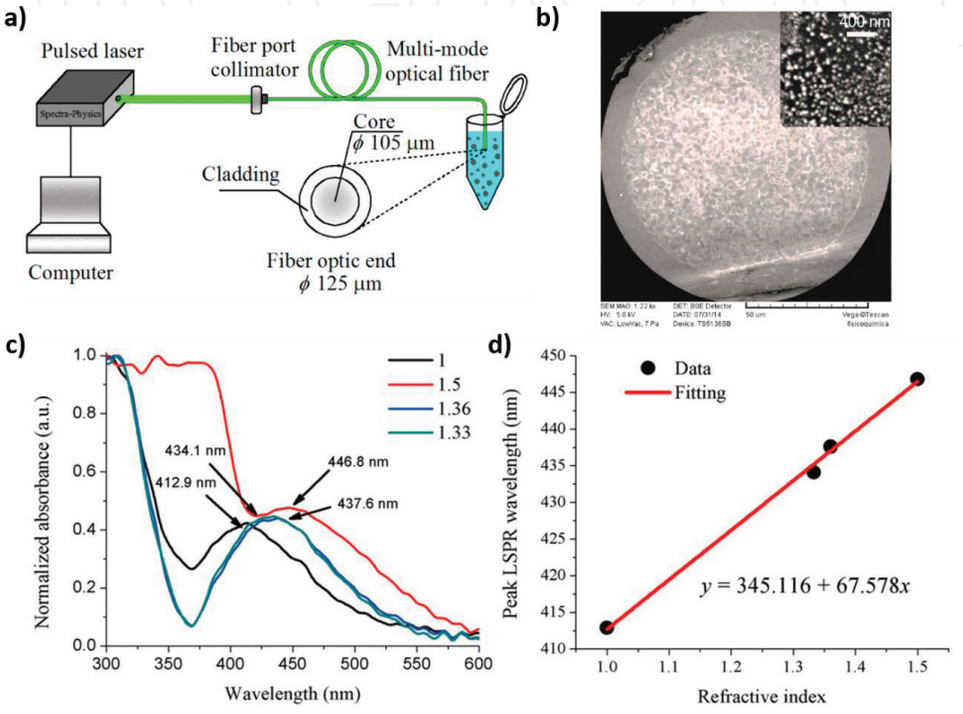

Figure 6. (a) Experimental setup for photodepositing silver nanoparticles on the optical fiber end; (b) image of the optical fiber end obtained with SEM; (c) sensor response localized in air, deionized water, ethanol and clove oil; (d) LSPR peak wavelength as a function of the refractive index. Reprinted with permission from Ref. [41].

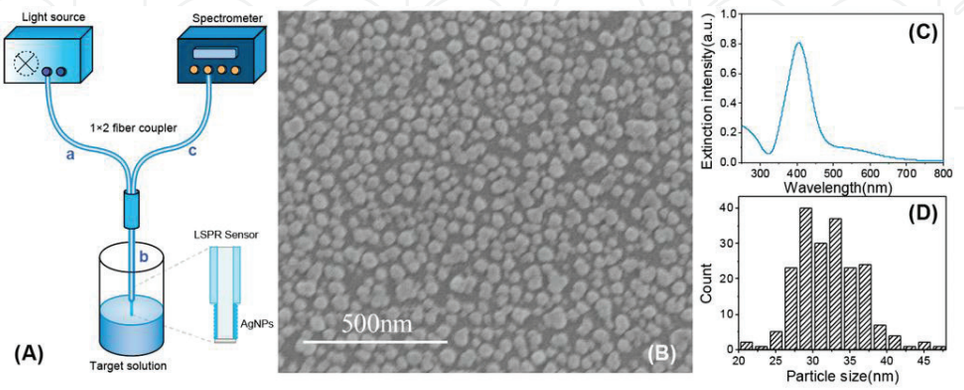

Figure 7. (A) Schematic of the experimental setup used in this study; (B) an SEM image of AgNPs after being immobilized on optical fiber; (C) absorption spectra of AgNPs solutions; (D) histogram showing the corresponding particle size distribution of AgNPs. Reprinted with permission [42].

http://dx.doi.org/10.5772/67544

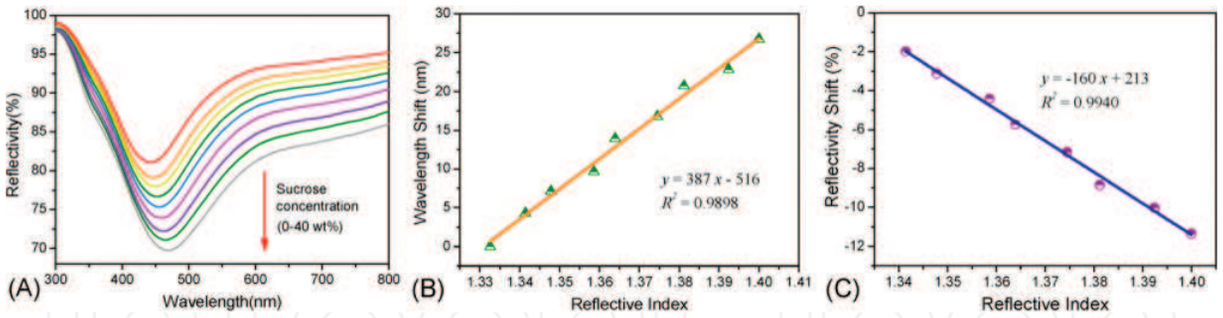

Figure 8. (A) The reflective spectra of the AgNP-based sensors of sucrose solutions with different concentrations; (B) changes in the LSPR wavelength shift to the refractive indices; (C) changes in the LSPR reflectivity shift to the refractive indices. Reprinted with permission [42].

between the amine groups on the fiber surface and negatively charged gold nanoparticles. The resulting LSPR peak wavelength position was located at 560 nm. An important consideration is that the sensitivity was found to be maximal when the bend diameter of the probe varies from 2 to 3 times the fiber diameter. The probes show sensitivity of 17.55 ($\Delta A_{560nm}/\Delta RIU$) in the visible region to refractive index changes from 1.33 to 1.47. Other approach based on a novel U-bent fiber optic probe is presented in Ref. [44]. In this work, U-bent probes with radii 0.5 and 0.75 mm have been coated with gold nanoparticles and tested with sucrose solution of variable RI with the aim to obtain information about the sensitivity and resolution. As a result, the best results were obtained for a bend radius of 0.75 mm with a sensitivity of 35 ($\Delta A_{540nm}/\Delta RIU$).

It is worth noting an interesting work of Cennamo et al. [45] using also a partially polished plastic optical fiber (POF). In this work, five-branched gold nanostars were synthesized with the peculiarity of showing three different localized surface plasmon resonances (known as LSPR1, LSPR2 and LSPR3). The strongest LSPRs (LSPR2 and LSPR3, respectively) fall in two well-separated spectral ranges. The first one (LSPR2) is located in the spectral range of 600–900 nm, whereas the second one (LSPR3) is located in the spectral range of 1100–1600 nm. However, due to the extremely strong attenuation of the employed POF in the infrared region, only the LSPR2 has been used for the RI measurements. The corresponding sensitivity is of 84 nm/RIU when the RI is ranging from 1.333 to 1.371, as it can be observed in **Figure 9**.

An interesting work is presented in Ref. [46], where a theoretical study is evaluated for the design of optical fiber sensors by using four different types of nanoparticles, such as ITO, Au, Ag and Cu. In this study, it has been assumed that all nanoparticles showed a spherical shape. The results have indicated that the sensitivity of LSPR-based fiber optic sensor increased with the increase in the thickness layer for all four materials. In addition, the simulation with ITO nanoparticles layer showed the better sensitivity in comparison with the other three materials.

A novel work for refractive index sensing is presented in Ref. [47]. In this work, a hetero-core structured fiber composed of a small section of single-mode fiber inserted in a multimode fiber is coated with gold nanoparticles using a simple, fast and low-cost method. The resultant sensor shows a sensitivity of 765 nm/RIU over a refractive index range of 1.333–1.365, and the points are fit to a linear plot with a square correlation coefficient value of 0.99, showing a

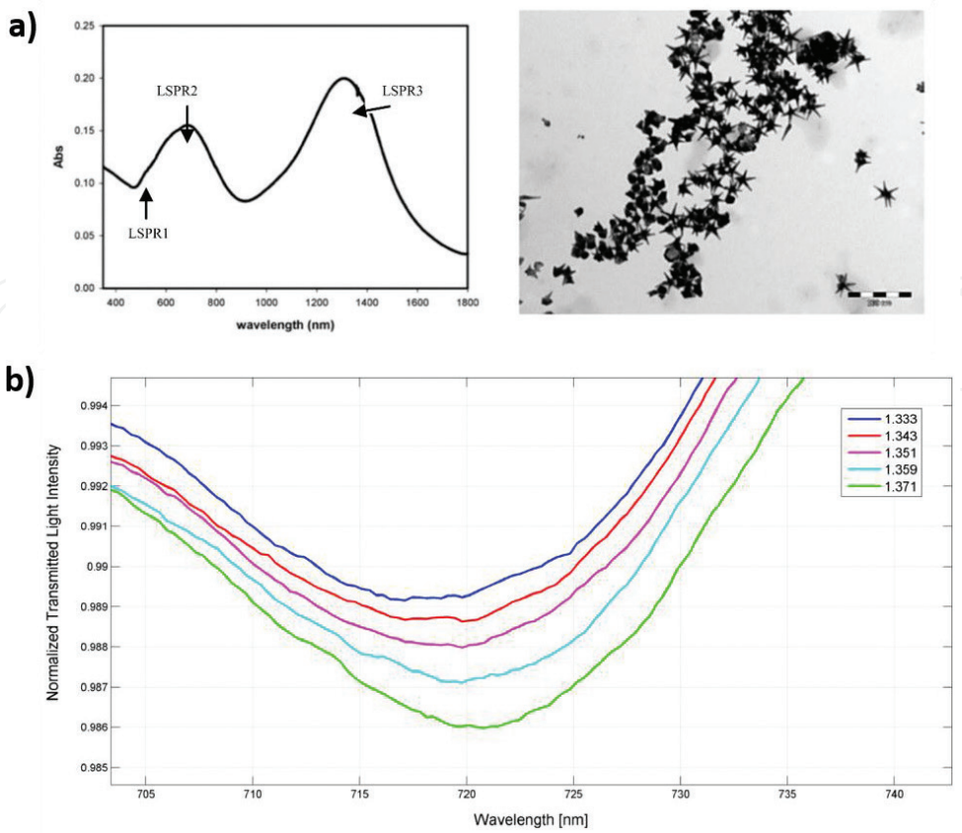

Figure 9. (a) UV-vis-NIR absorption spectrum of the five-branched gold nanostars with TEM image of the sample; (b) LSPR2 transmission spectra for different refractive indices of the aqueous solution medium. Reprinted with permission from Ref. [45].

resolution of 6.6×10^{-4}. It has to be mentioned that the sensor shows a high sensitivity, but it is necessary to obtain a better control over several parameters such as nanoparticle size, homogeneous distribution or even the cluster formation.

Interesting works with surprising results can be found in Refs. [48–52] using gold nanoparticles with different shapes. A study about the influence of the AuNPs size on the corresponding LSPR sensor sensitivity is evaluated in Ref. [48]. The main conclusion is that an increase in the sensitivity for the devices is obtained when the particle size is gradually increased. In this study, four different gold sizes (13, 20, 40 and 60 nm) have been investigated, and higher values in the resultant sensitivity have been observed (154 ± 14, 266 ± 27, 418 ± 44 and 571 ± 68 nm/RIU, respectively). A similar approach is presented in Ref. [49], although, in this work, the LSPR-based optical fiber sensitivity is evaluated using four types of gold nanorods (GNR) with different aspect ratios. The UV-vis spectra of the GNR solution reveal that by increasing the aspect ratio, a redshift of the longitudinal plasmon wavelength is appreciated. A first conclusion is that the transverse plasmon resonance (shorter wavelength location) only shows an increase in absorbance without wavelength shift when the refractive index is increased. However, the longitudinal plasmon resonance (longer wavelength location) shows both an increase in absorbance and wavelength redshift for higher values of refractive index. And a second conclusion is that by increasing

the aspect ratio (2.6, 3.1, 3.7 and 4.3) of the GNR, an increase in the resulting sensitivity of the LSPR sensors has been also obtained from 269, 401, 506 and 766 nm/RIU, respectively. Similar results about the different sensitivities of both transverse and longitudinal plasmon resonances are found in Ref. [50], being the longitudinal plasmon resonance very sensitive to RI changes in comparison with transverse plasmon resonance. In this work, the aspect ratio of the GNRs synthesized is approximately 3.5 and there is a total wavelength shift of 70 nm when the RI is varied from 1.333 to 1.423, showing a sensitivity of 778 nm/RIU.

Other interesting work based on the immobilization of GNR with a specific aspect ratio of 3 shows a sensitivity of 468 nm/RIU when the sensor is exposed to RI ranges from 1.33 to 1.3749 [51]. In this work, a redshift of the longitudinal plasmon resonance from the lowest to the highest RI value is also observed, and when the RI value is decreased, it is reversed with the corresponding blueshift.

Finally, a novel LSPR-based optical fiber sensor with a considerable improvement in the sensitivity for RI measurements is presented in Ref. [52]. In this work, the use of hollow gold nanoparticles has attracted the attention due to the stronger plasmonic effect in comparison with the use of solid gold nanoparticles. A main conclusion is that by increasing the resultant degree of hollowness of the gold structures, the sensitivity has been increased from 784 to 1933 nm/RIU, respectively.

In order to have a better understanding of the different LSPR-based optical fiber sensors used as refractometer as well as the type and shape of the corresponding nanoparticles immobilized in the optical fiber with their corresponding sensitivity, a summary is shown in **Table 1**.

Type of nanoparticles	Refractive index range	Sensitivity
Silver nanoparticles	From 1 to 1.5	67.6 nm/RIU [41]
Silver nanoparticles (spherical shape)	From 1.33 to 1.40	387 nm/RIU [42]
Gold nanoparticles (nanoflower shape)	From 1.33 to 1.47	17.55 ($\Delta A_{560nm}/\Delta RIU$) [43]
Gold nanoparticles	From 1.33 to 1.40	35 ($\Delta A_{540nm}/\Delta RIU$) [44]
Gold nanoparticles (nanostar shape)	From 1.333 to 1.371	84 nm/RIU [45]
Gold nanoparticles	From 1.333 to 1.365	765 nm/RIU [47]
Gold nanoparticles	From 1.333 to 1.424	571 nm/RIU [48]
Gold nanorods	From 1.34 to 1.41	766 nm/RIU [49]
Gold nanorods	From 1.333 to 1.423	778 nm/RIU [50]
Gold nanorods	From 1.33 to 1.3749	468 nm/RIU [51]
Hollow gold nanoparticles	From 1.333 to 1.407	1933 nm/RIU [52]

Table 1. Summary of the different types of nanoparticles used for the fabrication of LSPR-based optical fiber sensor with their corresponding sensitivities to refractive index changes.

4.1.2. Optical fiber humidity sensors

Nowadays, the design of optimal relative humidity (RH)-sensing devices is a big concern among scientific sensor community. This kind of devices has a great interest in a wide range of different fields, such as food quality preservation, gas purification, medical facilities or air-conditioning regulation. Due to this high number of applications in general industry, the development of sensing devices for monitoring RH has been increasing in industrial processing and environmental control [53].

As previously commented, one of the most used techniques at nanoscale level in order to obtain self-ordered nanostructures with a precise thickness control is the layer-by-layer assembly. One advantage of using this deposition process is the ability to place different kinds of nanoparticles throughout the multilayer polymeric films. The incorporation of silver nanoparticles inside LbL polymeric coating contributes to enhance the lifetime of the devices in high RH environments. In such RH conditions, the biocide behavior of AgNPs prevents the adverse bactericidal apparition, which could damage the sensitive coating [54–56].

In this sense, several articles have been very recently published based on the combination of AgNPs-loaded polymeric thin films with optical fiber devices to monitor relative humidity changes [57–59]. In initial studies of this research group, the changes in the RH ranging from 20 to 70% have been detected by a shift of the corresponding LSPR wavelength position [57, 58]. This aspect can be clearly observed in **Figure 10** where an optical fiber sensor consisting of a thickness of 15 bilayers of PAH/PAA-AgNPs using the LbL-E deposition technique has been fabricated (**Figure 10b**), being possible to appreciate only a LSPR absorption band (around 440 nm) which it is attributed to the natural optical resonance (LSPR) of the AgNPs with mostly a spherical shape. In addition, a change in the intensity of the LSPR absorption band is observed as RH is varied with a linear response (inset **Figure 10b**). However, when the thickness coating is increased up to 25 bilayers, new absorption bands known as lossy-mode resonance (LMR) [60, 61] are appreciated in the visible region. Rivero et al. [59] were the first research group in reporting optical fiber sensors based on both localized surface plasmon resonance (LSPR) and lossy-mode resonance (LMR) for monitoring humidity changes. The experimental results indicate that the use of AgNPs makes possible the alteration of the refractive index of the polymeric overlay, allowing an improvement of the sensitivity to RH, and also improving the visibility of the LMR band with a smaller thickness in comparison with a polymeric overlay without metallic nanoparticles [62]. In addition, there is an important difference in sensitivity related to both absorption peaks for humidity changes because LSPR band only shows a variation of 3 nm, while LMR band shows a considerable shift of 50 nm when the device is tested between 20 and 70% RH (see **Figure 10c**). Due to this high difference in sensitivity of the LMR band, the response time of the device has been also evaluated by exposing to quick RH changes (**Figure 10d**).

A similar work for monitoring quick RH changes such as human breathing is also presented in Ref. [63]. However, this work shows two significant differences in comparison with Ref. [59]. Firstly, the fabrication process is different because it is based on in situ synthesis (ISS) process of AgNPs inside a polymeric coating instead of using the LbL-E deposition technique.

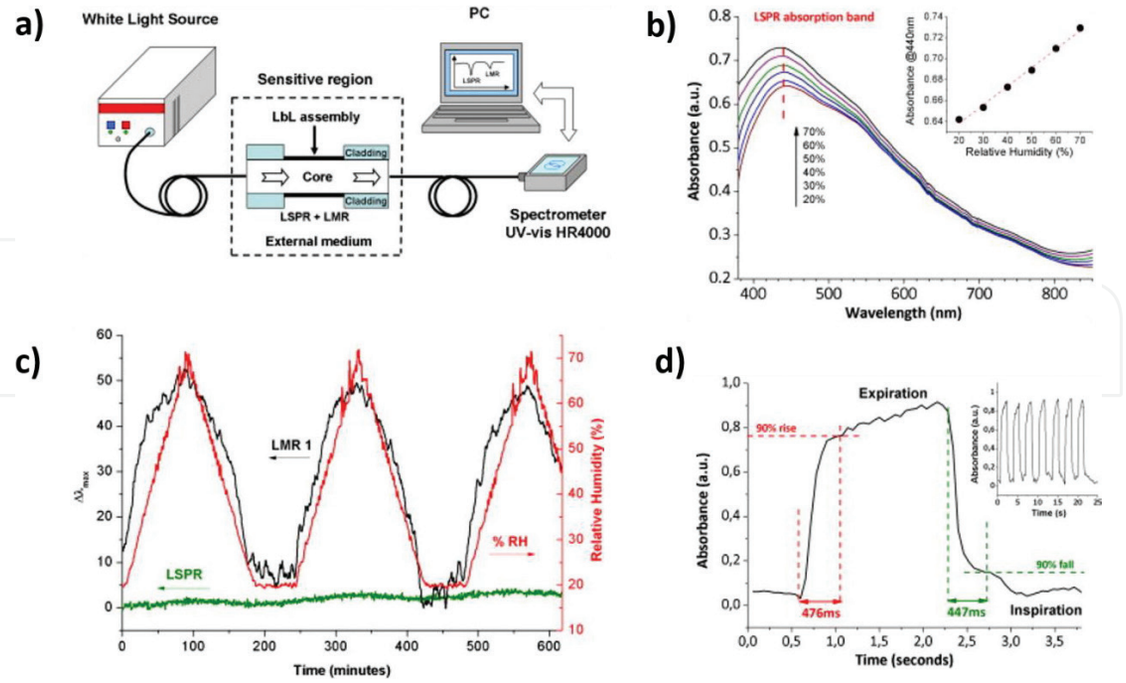

Figure 10. (a) Experimental setup used to obtain and characterize the absorption bands in the visible region; (b) UV-vis spectra when LbL-E of the silver nanoparticles is performed. The main absorption band is the LSPR corresponding to the AgNPs incorporated into the thin film. The curves plotted are 1, 3, 6, 9, 12 and 15 bilayers. (b) Spectral response of the device to RH ranges from 20 to 70% RH at a constant temperature of 25°C; (c) dynamic response of a 25 bilayers PAH/PAA-AgNPs device. The wavelength shift of both LSPR and LMR is monitored simultaneously to RH cycles from 20 to 70% RH at 25°C. (d) Response time of the device to several consecutive human breathing cycles (rise and fall). Reprinted with permission from Ref. [59] Elsevier (2012).

And secondly, the incorporation of AgNPs affects the refractive index of the overlay promoting the observation of a resonant attenuation band (LMR) in the infrared region (NIR). These results reveal that the combination of nanotechnology and biomedical science makes enable their use in practical RH monitoring applications or even it can lead to monitor high humidity changes such as human breathing due to the fast response time in the maximum sensitivity region.

4.2. Detection of chemical parameters

4.2.1. Optical fiber pH sensors

The polymeric structure presented in the LbL assembly (PAH/PAA) is not only sensitive to RH changes. In addition, if the specific nanocoating is dipped into liquid solutions, its thickness can be tuned by the external medium pH. This effect has been named "swelling/deswelling phenomenon" [64, 65]. As a consequence of this variation, the effective refractive index of the structure will change, producing a shift of the attenuation bands. In this sense, optical fiber resonance-based pH sensors using gold nanoparticles into polymeric layer-by-layer coatings have reported [66, 67]. These works are based on the design and fabrication of dual LSPR-LMR optical fiber pH sensors, using the LSPR band as a reference signal, and the LMR band is used as a sensing signal due to the great difference in their sensitivities to pH of

the surrounding medium. In addition, although previous works have been demonstrated the possibility of combining both phenomena in the same device by using AgNPs [59], the use of metallic gold nanoparticles (AuNPs) presents several additional advantages such as a great biocompatibility, nonreactivity, chemical stability and easiness to a further functionalization. In **Figure 11**, it can be clearly observed that the AuNPs have been successfully incorporated into the coatings by using LbL-E deposition technique because when the number of bilayers is increased, the resultant color of the films is changed from transparent to purple (inset **Figure 11a**). Once the nanocoating based on AuNPs is performed onto the optical fiber core by using LbL-E deposition technique, and the two optical phenomena (LSPR and LMR, respectively) are appreciated to a desired thickness coating, the spectral response of the device is measured at different pH values ranging from 4.0 to 6.0 (see **Figure 11b**) where it can be clearly observed the great difference in sensitivity of both absorption bands to these pH changes.

Other interesting approach based on the swelling/deswelling phenomenon related to a polymeric matrix is presented by Muri and Hjelme [68] for pH-sensing applications. In this work, a pH optical fiber sensor is fabricated based on LSPR sensing in a poly(acrylamide-co-acrylic acid) hydrogel embedding gold nanoparticles (GNP). As an interesting result, the LSPR absorption band is mainly shifted by two different processes. The first one is associated with an increase in the gold nanoparticles density in hydrogel when the pH solution is decreased, and as a result, the neighboring distances between GNP are decreased that can induce electromagnetic interactions between the localized modes, giving a LSPR redshift. The second one is associated with the density of the polymer matrix of the resultant hydrogel that is also increased when the pH solution is gradually decreased. In this case, a change in the refractive index around the AuNPs makes possible a shift of the LSPR absorption band.

4.2.2. Optical fiber sensors for detection of heavy metals

The detection and quantification of heavy metals is a hot topic in a large number of industrial, environmental and medical applications. In addition, it has been demonstrated that elevated

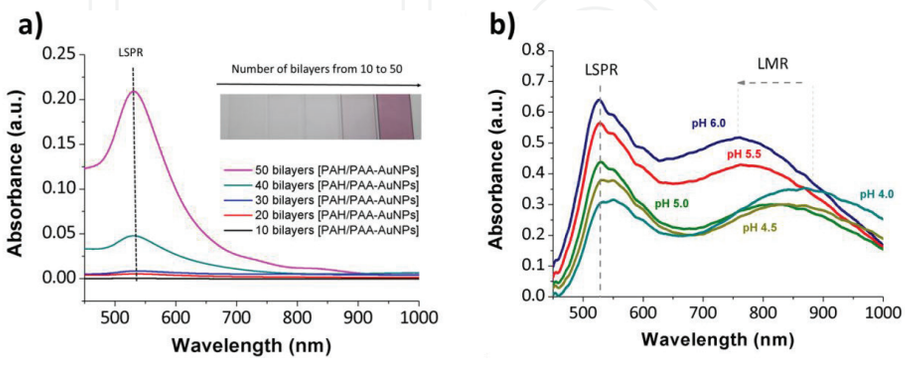

Figure 11. (a) UV-vis spectra of the nanostructured coating obtained by layer-by-layer embedding (LbL-E) deposition technique for different number of bilayers and a photograph of the resultant nanocoatings; (b) maximum wavelength variation of both LSPR and LMR absorption bands. The wavelength shift is monitored simultaneously at different pH values such as pH 4.0, pH 4.5, pH 5.0, pH 5.5 and pH 6.0, respectively. Reprinted with permission from Ref. [66]. Copyright (2016) Springer.

levels of heavy metals (lead, cadmium, mercury) in the human body can cause neurological disorders, such as birth defects, mental retardation or even death. Due to this, a great and precise control over these heavy metals is necessary for human safety o for environmental concern. For all these reasons, the development of optical fiber sensors for the detection of heavy metals can be a great alternative due to the possibility of real-time monitoring with a high degree of precision and a fast response.

An interesting study based on a fiber optic sensor for the detection of atmospheric elemental mercury can be found in Ref. [69] by using gold nanorods. In this work, the mercury readily is adsorbed on the gold nanorods and as a result, a shift related to the longitudinal plasmon resonance is appreciated. In addition, the experimental results indicate that a linear shift is obtained, which is directly proportional to the mercury concentration. The resultant optical fiber sensor can directly measure concentrations down to 1.0 $\mu g/m^3$.

Other promising works can be also found in the references for the detection of other different heavy metals by using LSPR-based fiber optical technology. As a characteristic example, Lin and Chung [70] have proposed a novel fiber optic biosensor to determine the heavy metal cadmium ion concentration. For this purpose, firstly, the preparation of gold nanoparticles and a further immobilization onto optical fiber is performed. And secondly, specific chelating agents known as phytochelatines (PCs) are immobilized onto gold nanoparticle-modified optical fiber. These agents play an important role because they are capable of chelating cadmium ions by thiolate coordination for a further sensing application. The experimental data indicate that the optical fiber sensor shows a maximal 9% change of absorbability for detecting 1–8 ppb of cadmium ions concentration. The resultant sensitivity is of 1.24 ppb with a limit of detection (LOD) of 0.16 ppb. In addition, an important consideration is that after successive cycles of deactivation and reactivation up to nine, the biosensor presents a good recovery rate with 85% original activity. In addition, one of the main characteristics of the sensor is that it can be recalibrated after storage in d-(+)-trehalose dehydrate solution. This same solution has been also used to recalibrate a biosensor for detecting lead ions [71]. However, the main difference with the previous work [70] is that a monoclonal antibody has been immobilized onto gold nanoparticle-modified optical fiber. A schematic representation of the functionalization of the optical fiber with the monoclonal antibody is presented in **Figure 12**.

As seen in this scheme, firstly, gold nanoparticles are immobilized onto optical fiber by using a silanization process with 3-(mercaptopropyl)-trimethoxysilane (MPTMS) in toluene. Then, by using a self-assembling technique, a bioactive layer composed of monoclonal antibody is immobilized by covalent coupling onto gold nanoparticle surface. For this purpose, a self-assembled layer of cystamine is initially performed to form amine functional groups onto gold nanoparticle surface. Then, the amine groups of cystamine can couple with the activated succimide esters (obtained from reaction between antibody and EDC/NHS), and as a result, the resultant antibodies are perfectly immobilized onto optical fiber surface. In addition, prior to detection process, the lead ions are treated with excess of chelators (i.e., EDTA) to form Pb-chelate complexes, Pb(II)-EDTA. Then, the monoclonal antibody can exclusively bind with this complex, causing a change in light attenuation. The experimental results indicate that the sensor shows a maximal 12% change of absorbability for detecting 10–100 ppb of

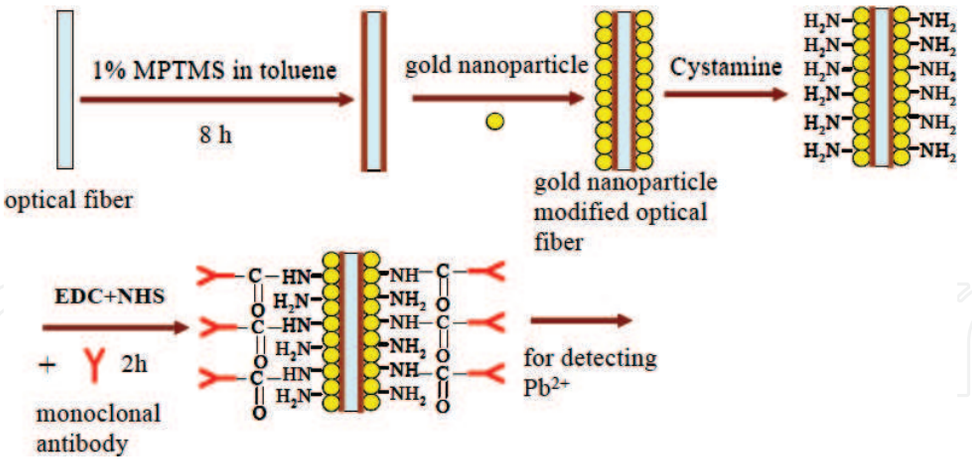

Figure 12. The chemical reactions scheme carried out for covalent binding of monoclonal antibody to the fiber-based LSPR sensor. Reprinted with permission from Ref. [71].

Pb(II)-EDTA complex concentration with a limit of detection (LOD) of 0.27 ppb. In addition, a very promising result is that the monoclonal antibody has a higher affinity to Pb(II)-EDTA in comparison with other chelate complexes such as Cu(II)-EDTA, Ni(II)-EDTA or Mg(II)-EDTA. The absorbability of these three chelate complexes is smaller (only 3% change) in comparison with Pb(II)-EDTA complex (12.2%). These experimental results can be appreciated in **Figure 13**.

4.2.3. Optical fiber sensors for detection of other chemical compounds

In this subsection, the use of LSPR-based optical fiber sensors is analyzed for the detection of different types of analytes of interest in fields as diverse as medicine, engineering, storage and food/drink industry. One of these analytes that is causing a great interest in the medical and clinical science is the hydrogen peroxide because it is a well-known reactive oxygen species (ROS) [72–74]. An excessive accumulation of this analyte in the body can trigger

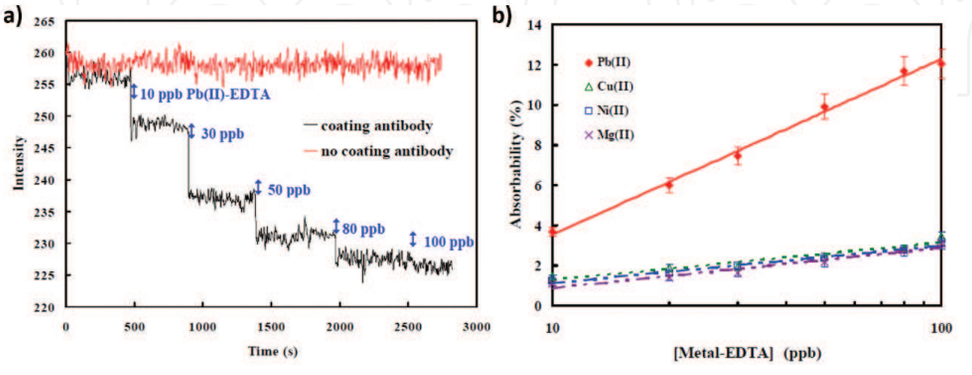

Figure 13. (a) An example of serial Pb(II)-EDTA complex response signal in the range of 10–100 ppb by two sensors with and without monoclonal antibody coating; (b) comparison of the responses between different metal-chelate complexes through the monoclonal antibody-functionalized LSPR sensor. Reprinted with permission from Ref. [71].

some diseases because the hydrogen peroxide is responsible for causing tissue damage and DNA fragmentation. There is a wide variety of techniques for its detection (spectrometry, fluorescence), although the use LSPR optical fiber sensors has the additional advantages of cost-effective, fast response and high sensitivity. An interesting approach is presented in Ref. [75] where a fiber optic sensor using the combined phenomena of both surface plasmon resonance (SPR) and localized surface plasmon resonance (LSPR) is fabricated for the detection of hydrogen peroxide. In this work, firstly, a silver layer is deposited onto an optical fiber core, and secondly, silver nanoparticles, which are embedded in a polymeric matrix of polyvinyl alcohol (PVA), are deposited over the silver-coated core of the optical fiber. The experimental results indicate that there is a redshift in the resonance wavelength when the hydrogen peroxide concentration is increased from 10^{-8} to 10^{-1} M. The resultant shift due to this combination (SPR + LSPR) is 29.401 nm, being this value higher in comparison with only SPR configuration (8.503 nm). Other approach based on this combined phenomena of SPR and LSPR can also be found in the references for the detection ascorbic acid [76].

Other interesting works based on the immobilization of metallic nanoparticles in a specific inorganic matrix are presented by using the sol-gel technology for sensing applications. As an example, sol-gel synthesis of palladium-doped silica nanocomposite (30 nm in diameter) has been successfully synthesized and incorporated onto fiber for hydrogen gas sensing [77]. The results indicate that the sensor shows response to the hydrogen gas (1% H_2 mixed with N_2 gas) and this response is reversible. Other approach based on the sol-gel technology for the detection of a harmful and corrosive analyte such as hydrofluoric acid (HF) is presented in Ref. [78]. For this purpose, a novel SiO_2 sol-gel-coating LSPR reflective sensor has been fabricated using gold nanoparticle-modified optical fibers. The results indicate that the sensors can detect HF solutions in the range from 1 to 5%. However, higher concentrations of HF are not possible to detect due to a quick erosion of the sensing area.

An interesting work for gasoline detection is presented in Ref. [79]. Gasoline is a fuel with a high volatile nature and a high degree of inflammability, which is necessary an adequate control over its storage. In this work, a comparative study about the difference in sensitivity of two different LSPR-based optical fiber sensors is presented for the detection of gasoline vapor concentration. The main difference in both sensors is that the first one is composed of only silver nanoparticles, whereas the second one is composed of only gold nanoparticles and both of them have been deposited on the decladed U-bent portion of a multimode fiber. The interaction between the sensing area and gasoline vapors at different concentrations has been monitored in a closed chamber. Finally, the experimental data indicate that the LSPR-based optical fiber based on AgNPs shows a better sensitivity than LSPR-based optical fiber based on AuNPs.

Finally, a novel work about the detection of sucrose content in fruit juices packaging industry is presented in Ref. [80] using a silicon nitride-coated LSPR-based fiber optic probe. This silicon nitride coating plays an important role because it is used to provide a protective layer on the device with the corresponding improvement in long-term stability for continuous operations. The results have demonstrated that there is 1.24 times RI sensitivity enhancement in case of metal nanoparticles (AuNPs) covered with silicon nitride film in comparison with only AuNPs-coated fiber optic probe.

4.3. Detection of biological parameters

In this section, optical fiber LSPR biosensors to perform qualitative and quantitative in real-time biomolecular sensing are presented. Several works are focused on the development of label-free biosensors because it is possible to monitor, with a high sensitivity and precision, the interaction between antibodies and their antigens in a wide number of sensing applications. As characteristic examples, biosensors for dengue diagnosis or for the detection of blood glucose are commented. In addition, the detection of the biotin-streptavidin bioconjugate pair or the IgG-anti-IgG bioreceptor-analyte pair is also analyzed for promising methods in applications as portable immunosensors.

One of the most known tropical diseases is the dengue, which can cause severe human health problems, and due to this, an early detection with an adequate therapy is one of the key factors for the human survival. For this purpose, the design and development of fiber optic sensors with AuNPs for dengue immunoassay can be found in Refs. [81, 82]. Different steps have been performed in order to immobilize a specific antibody (dengue anti-NS1) onto AuNPs deposited on the end surface of fiber [82]. Once a good immobilization of the sensing element onto AuNPs is obtained, a specular reflection LSPR optical fiber is performed for the detection of dengue NS1 antigen. The results indicate that the sensor is able to detect dengue NS1 antigen at different concentrations with a limit of detection of 1.54 nM.

Other approaches based on the same sensing mechanism by immobilization of metallic gold nanoparticles at the distal end of a multimode fiber can be found in Refs. [83–85]. As a characteristic example, the surface of gold nanorods has been functionalized with human IgG in order to create a biosensor to detect anti-human IgG [83]. The longitudinal peak has been used as sensing signal because a dependent shift was observed as a function of anti-human IgG concentration, being the limit of detection 3 nM. An improvement of the limit of detection for this same anti-human IgG is presented in Ref. [84]. In this work, a comparative study about the immobilization of two different types of gold nanoparticles such as nanospheres and nanorods onto an unclad surface of an optical fiber sensor and a further implementation as biosensors is evaluated. The results indicate that both biosensors present the same detection limit of 1.6 nM for the detection of anti-human IgG.

An interesting work for the detection of the biotin-streptavidin bioconjugate pair is presented in Ref. [85] using a reflective LSPR optical fiber. In this work, the layer-by-layer assembly (also known as ionic self-assembled multilayers, ISAM) has been used for obtaining a nanometric thickness composite, which is composed of gold nanoparticles and polyelectrolytes (see **Figure 14**). Finally, the experimental results have shown a wavelength shift as a function of the streptavidin concentration (see **Figure 15**), being the corresponding sensitivity of 800 pg/mm^2.

Other work based on the immobilization of silver nanoparticles instead of gold nanoparticles for the design of a reflective LSPR optical fiber biosensor is presented in Ref. [42]. An interesting result is that the resulting sensor shows a very high stability because a small fluctuation in resonance wavelength has been detected in a period of time of 18 days when the sensor was immersed in two different solutions such as ethanol and water (**Figure 16a**). In addition, the interaction between human IgG and rabbit anti-human IgG has been used as an analytical

model in order to evaluate the antigen-antibody interaction. The results indicate that a gradual shift of LSPR peak has been observed with an increase in the functionalized time (**Figure 16c**).

Other novel works based on the immobilization of bioreceptors during analyte binding onto the surface of gold nanoparticles can be also found in Refs. [44, 86–88]. These works are based on the absorbance or wavelength changes related to the gold nanoparticles using IgG-anti-IgG

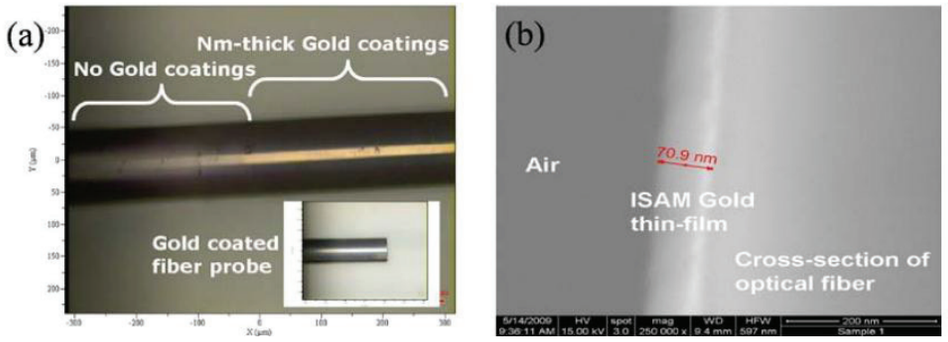

Figure 14. (a) photograph of gold metallic color in the portion of the fiber coated by ISAM; (b) cross section of the optical fiber in order to appreciate the nanometric thickness of the coating. Reprinted with permission from Ref. [85].

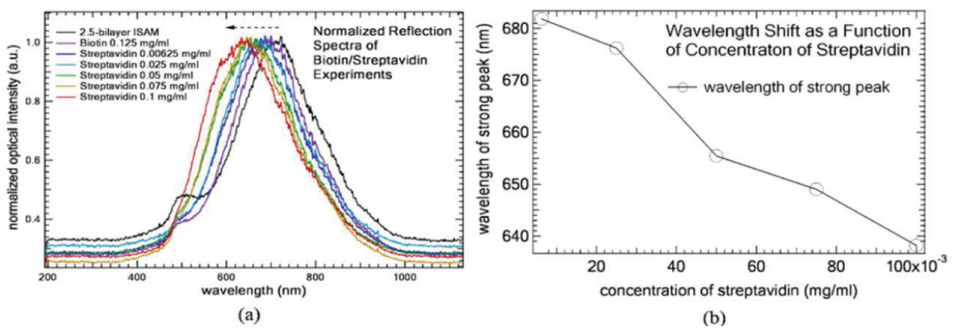

Figure 15. (a) Normalized reflection spectra measured in air as a function of the concentration of streptavidin solution using the same fiber optic probe; (b) wavelength shift as a function of concentration of streptavidin. Reprinted with permission from Ref. [85].

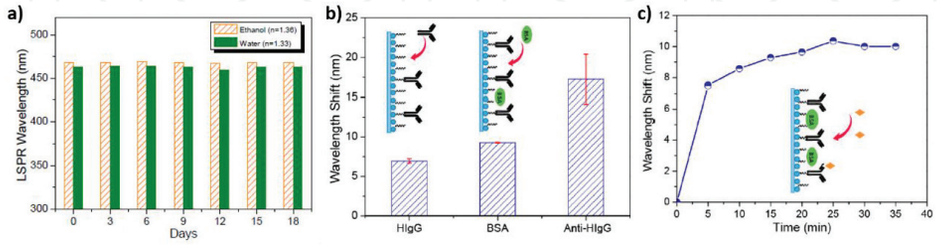

Figure 16. (a) LSPR wavelength monitoring of the AgNP-based sensor subjected in solutions with different refractive indices for a period of 18 days; (b) shifts of the LSPR spectra after different stages of surface modification relative to unmodified AgNP sensor probe; (c) LSPR peak wavelength changes during the process of anti-human IgG immobilization over a period of 35 min. Reprinted with permission from Ref. [42].

(bioreceptor-analyte pair) onto different optical fiber configurations. An approach is based on the design of novel U-bent optical fibers, which are able to detect a concentration of analyte of 0.8 nM (anti IgG) [44]. Other interesting work is presented in Ref. [86] where the optical fiber has been also bent in the form of a U-shaped probe for the detection of blood glucose. In addition, an interesting aspect is that the sensitivity of proposed biosensor has been evaluated as a function of the bending radius of the optical fiber.

Using this same configuration of U-bend fiber optic is presented in Ref. [87], although the resultant immobilization of the gold nanoparticles and IgG is performed in a multilayer structure using the layer-by-layer assembly. In this work, an exhaustive study about the plasmon penetration depth as a function of the resulting size of the AuNPs (18, 36 and 45 nm, respectively) is presented for the design of LSPR-based fiber optic biosensors. Other interesting work can be found in Ref. [88] where a tapered optical fiber sensor has been fabricated for monitoring anti-DNP antibody with a LOD of 4.8 pM.

Other optical fiber biosensor based on the layer-by-layer technique is also found in Ref. [89]. In this work, a gold nanoparticle-assembled film is used as a sensing layer, which has been built onto a trilayer polyelectrolyte structure-modified sidewall of an unclad optical fiber. The three consecutive polyelectrolytes used to form the trilayer structure are, firstly, a strong cationic polyelectrolyte (PDDA), secondly, a strong anionic polyelectrolyte (PSS) and, thirdly, a weak polyelectrolyte (PAH). After that, citrate-stabilized AuNPs have used to immobilize onto the outmost PAH layer. This multilayer structure is clearly appreciated in **Figure 17**. An important consideration of this sensing layer method is that a very time-saving compared is obtained in comparison with the assembly of AuNPs through silane-coupling process (silanization).

Once the gold nanoparticles have been successfully immobilized onto optical fiber surface, the LSPR optical fiber is modified by rabbit IgG in order to detect goat anti-rabbit IgG. In **Figure 18**, the dynamic process of goat anti-rabbit IgG adsorption is appreciated. In addition, first of all, it is necessary to remark that both rabbit IgG and goat anti-rabbit IgG cause a remarkable increase in the peak intensity. In addition, the experimental results also indicate that there is a gradual increase in the peak intensity when the goat anti-rabbit IgG concentration is increased. The lowest concentration that it can be detected for this biosensor is 11.1 ng/mL. Finally, this biosensor fabricated for this method shows potential application as a portable immunosensor.

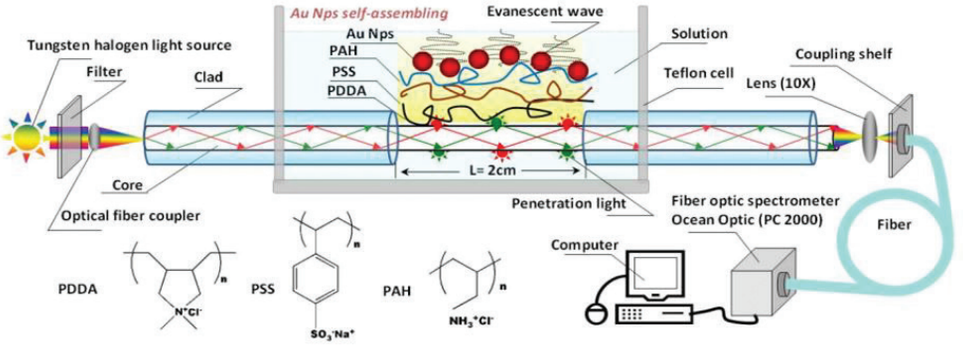

Figure 17. The experimental setup of the optical fiber LSPR sensor. Reprinted with permission from Ref. [89].

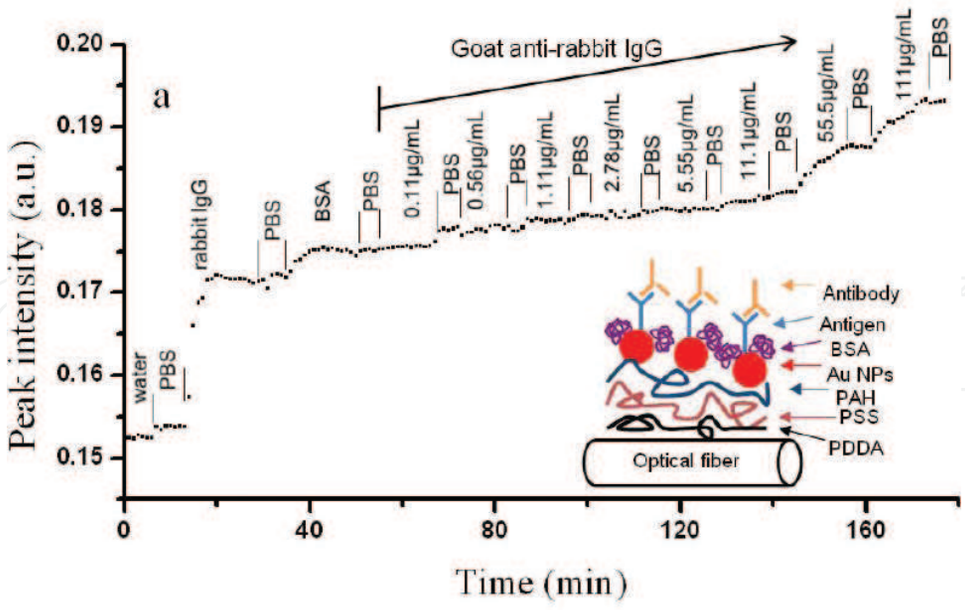

Figure 18. The LSPR biosensing of different concentrations of goat anti-rabbit IgG (0.11–100 μg/mL). Reprinted with permission from Ref. [89].

In a novel work [90], the detection limits of protein optical fiber biosensors coated with gold nanoparticles have been considerably improved. In this sense, a comparative study has been performed between a reference sensor without AuNPs and sensors composed of gold nanocages (AuNC) and nanospheres (AuNS), respectively. All the nanoparticles have been immobilized onto the fiber and the resulting sensor operated in a reflection mode. In this work, the sensor composed of AuNC showed a lower LOD and sensitivity than the sensor composed of AuNS. In addition, the LOD related to sensors composed of gold nanoparticles was three orders of magnitude greater than the reference sensor, showing the enhancement of the device due to the use of metal nanoparticles.

Finally, other promising biosensor of great and relevant interest is presented in Ref. [91]. In this work, a localized surface plasmon resonance (LSPR)-coupled fiber optic (FO) nanoprobe based on a gold nanodisk array at the fiber end facet is reported. This biosensor is capable of detecting a cancer protein biomarker, known as free prostate-specific antigen (f-PSA). The experimental data have demonstrated that the lowest limit of detection (LOD) was at 100 fg/mL (around 3 fM), showing an excellent specificity and selectivity in the resulting detection.

5. Conclusions

In this chapter, a review of the current state of the art of the LSPR-based optical fiber sensors is presented. LSPR has demonstrated to be a powerful tool for the development of high sensitivity optical sensors, and its combination with optical fibers has provided advanced sensors in many applications.

A large amount of research works reported the study about the synthesis and optical-sensing properties of immobilized metallic nanoparticles (typically gold or silver) as well as the influence of their composition, size, shape (spherical, nanorods, nanostars, nanoflowers, nanocages, etc.) or even solid or hollow core structure. Some authors have developed sensors based on thin-film-embedded metallic nanoparticles by means of layer-by-layer (LbL) and sol-gel techniques, whereas other authors have reported direct covalent binding of the nanoparticles to the optical fibers, using mostly silane-coupling processes.

Moreover, different optical configurations of the optical fiber sensors have been observed such as U-bent, transmission, reflection and optical fiber gratings. In each configuration, the metal nanoparticles have been immobilized over the optical fiber-sensitive region to detect the desired physical, chemical or biological parameters.

In summary, optical fibers provide a very powerful platform for optical sensing making possible the development of easy and robust optical measurements, remote sensing and lightweight devices. The use of LSPR in such optical fiber sensors enables to get fast and reliable measurements and very high-sensitivity devices with outstanding limit of detection (LOD) in the concentration range from nM to fM.

Acknowledgements

This work was supported by the Spanish Ministry of Economy and Competitiveness through TEC2013-43679-R Research Project.

Author details

Pedro J. Rivero[1*], Javier Goicoechea[2] and Francisco J. Arregui[2]

*Address all correspondence to: pedrojose.rivero@unavarra.es

1 Materials Engineering Laboratory, Department of Mechanical, Energetic and Materials Engineering, Public University of Navarre, Pamplona, Spain

2 Nanostructured Optical Devices Laboratory, Department of Electrical and Electronic Engineering, Public University of Navarre, Pamplona, Spain

References

[1] Federici, J. F.; Schulkin, B.; Huang, F.; Gary, D.; Barat, R.; Oliveira, F.; Zimdars, D. THz imaging and sensing for security applications—explosives, weapons and drugs. Semicond. Sci. Technol. 2005, 20, S266.

[2] Homola, J. Surface plasmon resonance sensors for detection of chemical and biological species. Chem. Rev. 2008, 108, 462-493.

[3] Fan, X.; White, I. M.; Shopova, S. I.; Zhu, H.; Suter, J. D.; Sun, Y. Sensitive optical biosensors for unlabeled targets: a review. Anal. Chim. Acta 2008, 620, 8-26.

[4] Mauter, M. S.; Elimelech, M. Environmental applications of carbon-based nanomaterials. Environ. Sci. Technol. 2008, 42, 5843-5859.

[5] Arregui, F. J.; Matias, I. R.; Goicoechea, J.; Villar, I. D. Optical fiber sensors based on nanostructured coatings. In Sensors Based on Nanostructured Materials; Ed. Springer. 2009; pp 275-301.

[6] Noguez, C. Surface plasmons on metal nanoparticles: the influence of shape and physical environment. J. Phys. Chem. C 2007, 111, 3606-3619.

[7] Anker, J. N.; Hall, W. P.; Lyandres, O.; Shah, N. C.; Zhao, J.; Van Duyne, R. P. biosensing with plasmonic nanosensors. Nat. Mater. 2008, 7, 442-453.

[8] Jeon, S.; Xu, P., Zhang, B.; MacK, N.H.; Tsai, H.; Chiang, L.Y.; Wang, H. Polymer-assisted preparation of metal nanoparticles with controlled size and morphology. J. Mater. Chem. 2011, 21, 2550-2554.

[9] Liz-Marzán L. M. Tailoring surface plasmons through the morphology and assembly of metal nanoparticles. Langmuir 2006, 22, 32-41.

[10] Zhao, J.; Zhang, X.; Yonzon, C. R.; Haes, A. J.; Van Duyne, R. P. Localized surface plasmon resonance biosensors. Nanomed 2006, 1, 219-228.

[11] Otte, M. A.; Sepúlveda, B.; Ni, W.; Juste, J. P.; Liz-Marzán, L. M.; Lechuga, L. M. Identification of the optimal spectral region for plasmonic and nanoplasmonic sensing. ACS Nano 2010, 4, 349-357.

[12] Liz-Marzán, L. M. Nanometals: formation and color. Mater. Today 2004, 7, 26-31.

[13] Angelomé, P. C.; Mezerji, H. H.; Goris, B.; Pastoriza-Santos, I.; Pérez-Juste, J.; Bals, S.; Liz-Marzán, L. M. Seedless synthesis of single crystalline Au nanoparticles with unusual shapes and tunable LSPR in the near-IR. Chem. Mater. 2012, 24, 1393-1399.

[14] Henry, A. I.; Bingham, J. M.; Ringe, E.; Marks, L. D.; Schatz, G. C.; Van Duyne, R. P. Correlated structure and optical property studies of plasmonic nanoparticles. J. Phys. Chem. C 2011, 115, 9291-9305.

[15] Mayer, K. M.; Hafner, J. H. Localized surface plasmon resonance sensors. Chem. Rev. 2011, 111, 3828-3857.

[16] Cobley, C. M.; Skrabalak, S. E.; Campbell, D. J.; Xia, Y. Shape-controlled synthesis of silver nanoparticles for plasmonic and sensing applications. Plasmonics 2009, 4, 171-179.

[17] Sepúlveda, B.; Angelomé, P. C.; Lechuga, L. M.; Liz-Marzán, L. M. LSPR-based nanobiosensors. Nano Today 2009, 4, 244-251.

[18] Rivero, P. J.; Goicoechea, J.; Urrutia, A.; Arregui, F. J. Effect of both protective and reducing agents in the synthesis of multicolor silver nanoparticles. Nanoscale Res. Lett. 2013, 8, 1-9.

[19] Hench, L. L.; West, J. K. The sol-gel process. Chem. Rev. 1990, 90, 33-72.

[20] Brinker, C. J.; Scherer, G. W. Sol → Gel → Glass: I. Gelation and gel structure. J. Non Cryst. Solids 1985, 70, 301-322.

[21] Brinker, C. J.; Scherer, G. W.; Roth, E. P. Sol → Gel → Glass: II. Physical and structural evolution during constant heating rate experiments. J. Non Cryst. Solids 1985, 72, 345-368.

[22] Scherer, G. W.; Brinker, C. J.; Roth, E. P. Sol → Gel → Glass: III. Viscous sintering. J. Non-Cryst. Solids 1985, 72, 369-389.

[23] Schmidt, H.; Scholze, H.; Kaiser, A. Principles of hydrolysis and condensation reaction of alkoxysilanes. J. Non Cryst. Solids 1984, 63, 1-11.

[24] Brinker, C. J. Hydrolysis and condensation of silicates: effects on structure. J. Non Cryst. Solids 1988, 100, 31-50.

[25] Sanchez, C.; Livage, J.; Henry, M.; Babonneau, F. Chemical modification of alkoxide precursors. J. Non Cryst. Solids 1988, 100, 65-76.

[26] Decher, G. Fuzzy nanoassemblies: toward layered polymeric multicomposites. Science 1997, 277, 1232-1237.

[27] Choi, J.; Rubner, M. F. Influence of the degree of ionization on weak polyelectrolyte multilayer assembly. Macromolecules 2005, 38, 116-124.

[28] Hammond, P. T. Form and function in multilayer assembly: new applications at the nanoscale. Adv. Mater. 2004, 16, 1271-1293.

[29] Shiratori, S. S.; Rubner, M. F. PH-dependent thickness behavior of sequentially adsorbed layers of weak polyelectrolytes. Macromolecules 2000, 33, 4213-4219.

[30] Budy, S. M.; Hamilton, D. J.; Cai, Y.; Knowles, M. K.; Reed, S. M. Polymer mediated layer-by-layer assembly of different shaped gold nanoparticles. J. Colloid. Interface Sci. 2017, 48, 336-347.

[31] Rivero, P. J.; Goicoechea, J.; Urrutia, A.; Matia, I. R.; Arregui, F. J. Multicolor Layer-by-Layer films using weak polyelectrolyte assisted synthesis of silver nanoparticles. Nanoscale Res. Lett. 2013, 8, 1-10.

[32] Rivero, P. J.; Goicoechea, J.; Matias, I. R.; Arregui, F. J. A comparative study of two different approaches for the incorporation of silver nanoparticles into layer-by-layer films. Nanoscale Res. Lett. 2014, 9, 1-11.

[33] Veletanlic, E.; Cynthia Goh, M. Polyelectrolyte multilayer films as templates for the in situ photochemical synthesis of silver nanoparticles. J. Phys. Chem. C 2009, 113, 18020-18026.

[34] Logar, M.; Jancar, B.; Šturm, S.; Suvorov, D. Weak polyion multilayer-assisted in situ synthesis as a route toward a plasmonic Ag/TiO_2 photocatalyst. Langmuir 2010, 26, 12215-12224.

[35] Arregui, F. J.; Dickerson, B.; Claus, R. O.; Matias, I. R.; Cooper, K. L. Polymeric thin films of controlled complex refractive index formed by the electrostatic self-assembled monolayer process. IEEE Photonics Technol. Lett. 2001, 13, 1319-1321.

[36] Cooper, P. R. Refractive-index measurements of liquids used in conjunction with optical fibers. Appl. Opt. 1983, 22, 3070-3072.

[37] Gouvêa, P. M. P.; Cancino-Bernardi, J.; Zucolotto, V.; Braga, A. M. B.; Carvalho, I. C. S. PAMAM dendrimer/gold nanoparticle nanocomposites for a reflection LSPR optical fiber sensor. In Proceedings of SPIE—The International Society for Optical Engineering; 2015; Vol. 9634.

[38] Rivero, P. J.; Hernaez, M.; Goicoechea, J.; Matias, I. R.; Arregui, F. J. Optical fiber refractometers based on localized surface plasmon resonance (LSPR) and lossy mode resonance (LMR). In Proceedings of SPIE—The International Society for Optical Engineering; 2014; Vol. 9157.

[39] Rivero, P. J.; Hernaez, M.; Goicoechea, J.; Matías, I. R.; Arregui, F. J. A comparative study in the sensitivity of optical fiber refractometers based on the incorporation of gold nanoparticles into layer-by-layer films. Int. J. Smart Sens. Intell. Syst. 2015, 8, 822-841.

[40] Sandhu, P.; Yang, J.; Xu, C. Q. In-fiber michelson interferometer with polymeric/nanoparticle thin-film overlay as a platform for biosensing. IEEE J. Sel. Top Quantum Electron 2010, 16, 685-690.

[41] Ortega-Mendoza, J. G.; Padilla-Vivanco, A.; Toxqui-Quitl, C.; Zaca-Morán, P.; Villegas-Hernández, D.; Chávez, F. Optical fiber sensor based on localized surface plasmon resonance using silver nanoparticles photodeposited on the optical fiber end. Sensors 2014, 14, 18701-18710.

[42] Chen, J.; Shi, S.; Su, R.; Qi, W.; Huang, R.; Wang, M.; Wang, L.; He, Z. Optimization and application of reflective LSPR optical fiber biosensors based on silver nanoparticles. Sensors 2015, 15, 12205-12217.

[43] Gowri, A.; Sai, V. V. R. Development of LSPR based U-bent plastic optical fiber sensors. Sens. Actuators B Chem. 2016, 230, 536-543.

[44] Sai, V. V. R.; Kundu, T.; Mukherji, S. Novel U-bent fiber optic probe for localized surface plasmon resonance based biosensor. Biosens. Bioelectron. 2009, 24, 2804-2809.

[45] Cennamo, N.; D'Agostino, G.; Donà, A.; Dacarro, G.; Pallavicini, P.; Pesavento, M.; Zeni, L. Localized surface plasmon resonance with five-branched gold nanostars in a plastic optical fiber for bio-chemical sensor implementation. Sensors 2013, 13, 14676-14686.

[46] Rani, M.; Sharma, N. K.; Sajal, V. Localized surface plasmon resonance based fiber optic sensor with nanoparticles. Opt. Commun. 2013, 292, 92-100.

[47] García, J. A.; Monzón-Hernández, D.; Manríquez, J.; Bustos, E. One step method to attach gold nanoparticles onto the surface of an optical fiber used for refractive index sensing. Opt. Mater. 2016, 51, 208-212.

[48] Tu, M. H.; Sun, T.; Grattan, K. T. V. Optimization of gold-nanoparticle-based optical fibre surface plasmon resonance (SPR)-based sensors. Sens. Actuators B Chem. 2012, 164, 43-53.

[49] Cao, J.; Galbraith, E. K.; Sun, T.; Grattan, K. T. V. Cross-comparison of surface plasmon resonance-based optical fiber sensors with different coating structures. IEEE Sensors J. 2012, 12, 2355-2361.

[50] Cao, J.; Galbraith, E.; Sun, T.; Grattan, K. T. V. Development and sensitivity studies of a gold nanorod platform for a localized surface plasmon resonance based optical fibre biosensor. In Proceedings of SPIE—The International Society for Optical Engineering; 2011; pp. 7753.

[51] Li, L.; Liang, Y.; Xie, L.; Lu, M.; Peng, W. Optical fiber surface plasmon resonance sensor with surface modified gold nanorods for biochemical detection. In Proceedings of SPIE—The International Society for Optical Engineering; 2014; Vol. 9277.

[52] Tu, M. H.; Sun, T.; Grattan, K. T. V. LSPR optical fibre sensors based on hollow gold nanostructures. Sens. Actuators, B Chem. 2014, 191, 37-44.

[53] Chen, Z.; Lu, C.; Grattan, K. T. V. Humidity sensors: a review of materials and mechanisms. Sensors 2005, 3, 274-295.

[54] Sharma, V. K.; Yngard, R. A.; Lin, Y. Silver nanoparticles: green synthesis and their antimicrobial activities. Adv. Colloid Interface Sci. 2009, 145, 83-96.

[55] Ilic, V.; Šaponjic, Z.; Vodnik, V.; Molina, R.; Dimitrijevic, S.; Jovancic, P.; Nedeljkovic, J.; Radetic, M. Antifungal efficiency of corona pretreated polyester and polyamide fabrics loaded with Ag nanoparticles. J. Mater. Sci. 2009, 44, 3983-3990.

[56] Rivero, P. J.; Urrutia, A.; Goicoechea, J.; Zamarreño, C. R.; Arregui, F. J.; Matías, I. R. An antibacterial coating based on a polymer/sol-gel hybrid matrix loaded with silver nanoparticles. Nanoscale Res. Lett. 2011, 6, X1–X7.

[57] Rivero, P. J.; Urrutia, A.; Goicoechea, J.; Arregui, F. J.; Matías, I. R. Humidity sensor based on silver nanoparticles embedded in a polymeric coating. In Proceedings of the 5th International Conference on Sensing Technology, ICST 2011, Palmerston North (New Zealand); 2011.

[58] Rivero, P. J.; Urrutia, A.; Goicoechea, J.; Arregui, F. J.; Matías, I. R. Humidity sensor based on silver nanoparticles embedded in a polymeric coating. Int. J. Smart Sensing Intell. Syst. 2012, 5, 71-83.

[59] Rivero, P. J.; Urrutia, A.; Goicoechea, J.; Arregui, F. J. Optical fiber humidity sensors based on localized surface plasmon resonance (LSPR) and Lossy-mode resonance (LMR) in overlays loaded with silver nanoparticles. Sens. Actuators B Chem. 2012, 173, 244-249.

[60] Del Villar, I.; Hernaez, M.; Zamarreno, C. R.; Sánchez, P.; Fernández-Valdivielso, C.; Arregui, F. J.; Matias, I. R. Design rules for Lossy mode resonance based sensors. Appl. Opt. 2012, 51, 4298-4307.

[61] Del Villar, I.; Zamarreño, C. R.; Sanchez, P.; Hernaez, M.; Valdivielso, C. F.; Arregui, F. J.; Matias, I. R. Generation of Lossy mode resonances by deposition of high-refractive-index coatings on uncladded multimode optical fibers. J. Optics 2010, 12, 095503.

[62] Zamarreño, C. R.; Hernáez, M.; Del Villar, I.; Matías, I. R.; Arregui, F. J. Optical fiber pH sensor based on Lossy-mode resonances by means of thin polymeric coatings. Sens. Actuators B Chem. 2011, 155, 290-297.

[63] Rivero, P. J.; Urrutia, A.; Goicoechea, J.; Matias, I. R.; Arregui, F. J. A Lossy mode resonance optical sensor using silver nanoparticles-loaded films for monitoring human breathing. Sens. Actuators B Chem. 2012, 187, 40-44.

[64] Goicoechea, J.; Zamarreño, C. R.; Matías I. R.; Arregui, F. J. Optical fiber pH sensors based on layer-by-layer electrostatic self-assembled Neutral Red. Sens. Actuators B Chem. 2008, 132, 305-311.

[65] Itano, K.; Choi, J.; Rubner, M. F. Mechanism of the pH-induced discontinuous swelling/deswelling transitions of poly(allylamine hydrochloride)-containing polyelectrolyte multilayer films. Macromolecules 2005, 38, 3450-3460.

[66] Rivero, P. J.; Goicoechea, J.; Hernaez, M.; Socorro; A. B.; Matias, I. R.; Arregui, F. J. Optical fiber resonance based-pH sensors using gold nanoparticles into polymeric layer-by-layer coatings. Microsyst. Technol. 2016, 22, 1821-1829.

[67] Socorro, A.B.; Rivero, P. J.; Hernaez, M.; Goicoechea, J.; Matias, I. R.; Arregui, F. J. Optical fiber pH sensor based on gold nanoparticles into polymeric coatings. In Proceedings of SPIE—The International Society for Optical Engineering; 2015; Vol. 9517.

[68] Muri H. I. D. I.; Hjelme D. R. Novel localized surface plasmon resonance based optical fiber sensor. In Progr Biomed Opt Imaging Proc SPIE; 2016; pp 9702.

[69] Crosby, J. S.; Lucas, D.; Koshland, C. P. Fiber optic based evanescent wave sensor for the detection of elemental mercury utilizing gold nanorods. Sens. Actuators B Chem. 2013, 181, 938-942.

[70] Lin, T. J.; Chung, M. F. Detection of cadmium by a fiber-optic biosensor based on localized surface plasmon resonance. Biosens. Bioelectron. 2009, 24, 1213-1218.

[71] Lin, T. J.; Chung, M. F. Using monoclonal antibody to determine lead ions with a localized surface plasmon resonance fiber-optic biosensor. Sensors 2008, 8, 582-593.

[72] Teerasong, S.; Sani, M.; Numsawat, P.; Martchoo, R.; Chompoosor, A.; Nacapricha, D. A silver nanoparticle thin film modified glass substrate as a colourimetric sensor for hydrogen peroxide. J. Exp. Nanosci. 2015, 10, 1327-1335.

[73] Gavrilenko, N. A.; Saranchina, N. V.; Gavrilenko, M. A. Colorimetric sensor based on silver nanoparticle—embedded polymethacrylate matrix. Adv. Mater. Res. 2014, 1040, 923-927.

[74] Hu, L.; Yuan, Y.; Zhang, L.; Zhao, J.; Majeed, S.; Xu, G. Copper nanoclusters as peroxidase mimetics and their applications to H_2O_2 and glucose detection. Anal. Chim. Acta 2013, 762, 83-86.

[75] Bhatia, P.; Yadav, P.; Gupta, B. D. Surface plasmon resonance based fiber optic hydrogen peroxide sensor using polymer embedded nanoparticles. Sens. Actuators B Chem. 2013, 182, 330-335.

[76] Shrivastav, A. M.; Usha, S. P.; Gupta, B. D. A Localized and propagating SPR, and molecular imprinting based fiber-optic ascorbic acid sensor using an in situ polymerized polyaniline-Ag nanocomposite. Nanotechnology 2016, 27, 345501.

[77] Guo, H.; Tao, S. Sol-gel synthesis of palladium-doped silica nanocomposite fiber using triton X-100 micelle template and the application for hydrogen gas sensing. IEEE Sens. J. 2007, 7, 323-328.

[78] Chen, I.; Lin, S. S.; Lin, T. J.; Du, J. K.. Detection of hydrofluoric acid by a SiO_2 sol-gel coating fiber-optic probe based on reflection-based localized surface plasmon resonance. Sensors 2011, 11, 1907-1923.

[79] Paul, D.; Dutta, S.; Biswas, R. LSPR enhanced gasoline sensing with a U-bent optical fiber. J. Phys. D 2016, 49, 305104.

[80] Chauhan, S. K.; Punjabi, N.; Sharma, D. K.; Mukherji, S. A silicon nitride coated LSPR based fiber-optic probe for possible continuous monitoring of sucrose content in fruit juices. Sens. Actuators B Chem. 2014, 222, 1240-1250.

[81] Camara, A. R.; Dias, A. C. M. S.; Gouvêa, P. M. P.; Braga, A. M. B.; Dutra, R. F.; De Araujo, R. E.; Carvalho, I. C. S. Fiber optic sensor with au nanoparticles for dengue immunoassay. In Optics InfoBase Conference Papers; 2013.

[82] Camara, A. R.; Gouvêa, P. M. P.; Dias, A. C. M. S.; Braga, A. M. B.; Dutra, R. F.; De Araujo, R. E.; Carvalho, I. C. S. Dengue immunoassay with an LSPR fiber optic sensor. Opt. Express 2013, 21, 27023-27031.

[83] Cao, J.; Sun, T.; Grattan, K. T. V. Development of gold nanorod-based localized surface plasmon resonance optical fiber biosensor. In Proceedings of SPIE—The International Society for Optical Engineering; 2012; Vol. 8421.

[84] Cao, J.; Tu, M. H.; Sun, T.; Grattan, K. T. V. Wavelength-based localized surface plasmon resonance optical fiber biosensor. Sens. Actuators B Chem. 2013, 181, 611-619.

[85] Wan, M.; Luo, P.; Jin, J.; Xing, J.; Wang, Z.; Wong, S. T. C. Fabrication of localized surface plasmon resonance fiber probes using ionic self-assembled gold nanoparticles. Sensors 2010, 10, 6477-6487.

[86] Srivastava, S. K.; Arora, V.; Sapra, S.; Gupta, B. D. Localized surface plasmon resonance-based fiber optic U-shaped biosensor for the detection of blood glucose. Plasmonics 2012, 7, 261-268.

[87] Bharadwaj, R.; Mukherji, S.; Mukherji, S. Probing the localized surface plasmon field of a gold nanoparticle-based fibre optic biosensor. Plasmonics 2016, 11, 753-761.

[88] Lin, H. Y.; Huang, C. H.; Cheng, G. L.; Chen, N. K.; Chui, H. C. Tapered optical fiber sensor based on localized surface plasmon resonance. Opt. Express 2012, 20, 21693-21701.

[89] Shao, Y.; Xu, S.; Zheng, X.; Wang, Y.; Xu, W. Optical fiber LSPR biosensor prepared by gold nanoparticle assembly on polyelectrolyte multilayer. Sensors 2010, 10, 3585-3596.

[90] Lepinay, S.; Staff, A.; Ianoul, A.; Albert, J. Improved detection limits of protein optical fiber biosensors coated with gold nanoparticles. Biosens. Bioelectron. 2014, 52, 337-344.

[91] Sanders, M.; Lin, Y.; Wei, J.; Bono, T.; Lindquist, R. G. An enhanced LSPR fiber-optic nanoprobe for ultrasensitive detection of protein biomarkers. Biosens. Bioelectron. 2014, 61, 95-101.

IntechOpen

IntechOpen